

Epigenetic status of argininosuccinate synthetase and argininosuccinate lyase modulates autophagy and cell death in glioblastoma

N Syed^{1*}, J Langer¹, K Janczar¹, P Singh¹, C Lo Nigro², L Lattanzio², HM Coley³, E Hatzimichael⁴, J Bomalaski⁵, P Szlosarek⁶, M Awad⁷, K O'Neil⁷, F Roncaroli¹ and T Crook⁸

Arginine deprivation, either by nutritional starvation or exposure to ADI-PEG20, induces adaptive transcriptional upregulation of *ASS1* and *ASL* in glioblastoma multiforme *ex vivo* cultures and cell lines. This adaptive transcriptional upregulation is blocked by neoplasia-specific CpG island methylation in either gene, causing arginine auxotrophy and cell death. In cells with methylated *ASS1* or *ASL* CpG islands, ADI-PEG20 initially induces a protective autophagic response, but abrogation of this by chloroquine accelerates and potentiates cytotoxicity. Concomitant methylation in the CpG islands of both *ASS1* and *ASL*, observed in a subset of cases, confers hypersensitivity to ADI-PEG20. Cancer stem cells positive for CD133 and methylation in the *ASL* CpG island retain sensitivity to ADI-PEG20. Our results show for the first time that epigenetic changes occur in both of the two key genes of arginine biosynthesis in human cancer and confer sensitivity to therapeutic arginine deprivation. We demonstrate that methylation status of the CpG islands, rather than expression levels *per se* of the genes, predicts sensitivity to arginine deprivation. Our results suggest a novel therapeutic strategy for this invariably fatal central nervous system neoplasm for which we have identified robust biomarkers and which overcomes the limitations to conventional chemotherapy imposed by the blood/brain barrier.

Cell Death and Disease (2013) 4, e458; doi:10.1038/cddis.2012.197; published online 17 January 2013

Subject Category: Cancer

Glioblastoma multiforme (GBM) is the most common primary human malignant brain tumour and is among the most lethal of all cancers.¹ Despite advances in surgical management and radiotherapy, and development of temozolomide, the median survival for patients is 12–16 months.^{2,3} The unfavourable prognosis in this disease is strongly correlated to the intrinsic apoptosis resistance of GBM.^{4,5} Disease recurrence after treatment is mechanistically linked to the presence of chemo-/radio-resistant CD133⁺ cancer stem cells (CSCs).⁶ A further barrier to effective therapy of GBM is the presence of the blood/brain barrier, which limits access of chemotherapy to the central nervous system. These considerations clearly underline the urgent need for novel therapeutic approaches. GBM cells are less sensitive to apoptosis,⁴ yet less resistant to therapies that induce autophagy.^{7–9} Temozolomide, the most active agent in treating GBM, exerts cytotoxicity by inducing autophagic cell death.¹⁰ Autophagy is a non-apoptotic route of programmed cell death involving the formation of large

double-membrane autophagic vacuoles termed autophagosomes^{11,12} to degrade and recycle long-lived organelles and proteins by merging with lysosomes to form autolysosomes. Autophagy has a critical role in cellular survival during periods of starvation, but when stress conditions are excessive, autophagy becomes a cellular suicide pathway. As such, autophagy is initially an adaptive response to ensure survival but beyond a certain threshold may mediate a form of non-caspase-mediated cell death.

Tumour cells have a high requirement for arginine. This semi-essential amino acid is synthesized from citrulline via the urea cycle enzymes argininosuccinate synthetase (ASS) and argininosuccinate lyase (ASL).¹³ In a subset of human cancers, ASS expression is lost rendering them highly sensitive to deprivation of arginine by pegylated arginine deiminase (ADI-PEG20).^{14–21} ADI-PEG20 induces autophagic cell death in melanoma and in prostate carcinoma.^{18,22} ASS and ASL are tightly coupled and upregulated

¹John Fulcher Neuro-oncology laboratory, Division of Brain Sciences, Faculty of Medicine, Imperial College London, London W6 8RP, UK; ²Laboratory of Cancer Genetics and Translational Oncology, S. Croce General Hospital, Cuneo, Italy; ³Faculty of Health and Medical Sciences, University of Surrey, Surrey GU2 7XH, UK; ⁴Hematology Research Laboratory, University Hospital of Ioannina, Ioannina, Greece; ⁵Polaris Pharmaceuticals Inc., 9373 Towne Centre Drive, Suite 150, San Diego, CA, USA; ⁶Barts Cancer Institute, Queen Mary University of London, Centre for Molecular Oncology, Charterhouse Square, London, UK; ⁷Department of Neurosurgery, Charing Cross Hospital, London W6 8RF, UK and ⁸Division of Cancer Research, Medical Research Institute, University of Dundee, Ninewells Hospital and Medical School, Dundee DD1 9SY, UK

*Corresponding author: N Syed, John Fulcher Neuro-oncology laboratory, Division of Brain Sciences, Faculty of Medicine, Imperial College London, London W6 8RP, UK. Tel: +44 0208 846 7029; Fax: +44 0208 846 7794; E-mail: n.syed@imperial.ac.uk

Keywords: glioblastoma; arginine; epigenetics; argininosuccinate synthetase; argininosuccinate lyase; autophagy

Abbreviations: ASL, argininosuccinate lyase; ASS, argininosuccinate synthetase; ADI-PEG20, arginine deiminase PEG20; 5'AZA, 5-Aza-2'-deoxycytidine; GBM, glioblastoma multiforme; qPCR, quantitative PCR; CSC, cancer stem cell; MSP, methylation-specific PCR; SRB, sulphorodamine B; CQ, chloroquine

Received 15.6.12; revised 03.11.12; accepted 26.11.12; Edited by P Salomoni

in activated rat microglia,^{23,24} implying that both genes are dynamically controlled according to cellular stresses. So far, no reports of ASL-negative cancers have been documented.

Previous studies have identified a number of genes subject to methylation-dependent transcriptional silencing in high-grade brain tumours.^{25–27} To seek additional epigenetically regulated genes in GBM, we performed methylation reversal and micro-array analysis in GBM cell lines. Here, we describe the identification and characterization of the two key enzymes in arginine biosynthesis, *ASS1* and *ASL*, as epigenetically regulated genes in GBM, and we demonstrate that epigenetic changes in these changes modulate cellular sensitivity to therapeutic autophagy.

Results

Methylation reversal identifies novel methylated genes in GBM. We used 5-Aza-2'-deoxycytidine (5'AZA) to reverse transcriptional silencing in the GAMG GBM cell line. mRNAs upregulated by demethylation were identified by micro-array analysis. The mRNA of 47 genes was upregulated at least twofold by 5'AZA and of 791 genes at least 1.4-fold. We selected 10 genes and confirmed upregulation by 5'AZA for 7 of them (Figure 1a). Among the genes

upregulated by 5'AZA in GAMG cells was *ASS1*, which contains a CpG island in the 5' regulatory sequences of the gene (see Supplementary Figure S1 for map of CpG island, including location of primers). This gene encodes ASS, the enzyme catalysing the rate-limiting step in arginine biosynthesis. Using quantitative PCR (qPCR) and western blotting, we confirmed upregulation of *ASS1* mRNA by 5'AZA in the GAMG cell line but not in the 42MG cell line (Figure 1b). Using methylation-specific PCR (MSP), we confirmed that the increased expression of *ASS1* in GAMG following 5'AZA is accompanied by a decrease in CpG island methylation that does not occur in 42MG (Figure 1b).

Silencing of *ASS1* in primary cultures of GBM. To investigate in detail the potential epigenetic regulation of *ASS1*, we established 22 primary GBM cultures from tissue obtained at first surgical debulking of patients in our clinical practice. These early passage cultures were tested for expression and methylation of *ASS1*. Downregulation of *ASS1* mRNA and protein was observed in 8/22 cases, results are shown for 10 cases (Figure 1c). Using MSP and pyrosequencing, all cases with *ASS1* methylation had downregulation of *ASS1* mRNA (GBM 31, 53 and 59). However, in some cases, *ASS1* mRNA was downregulated

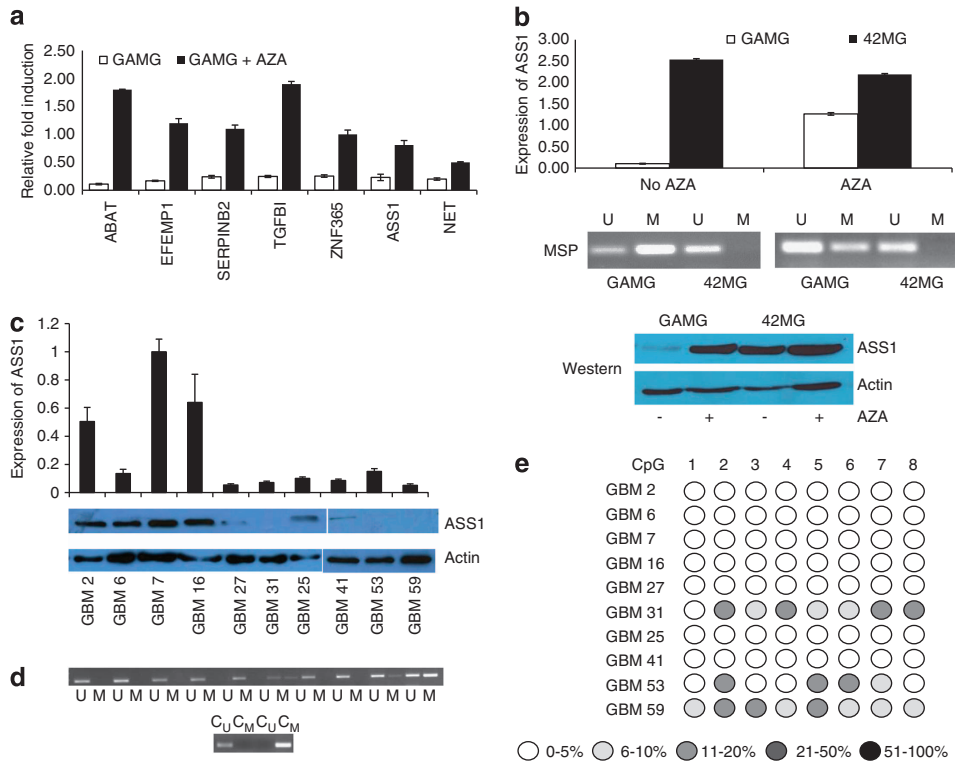


Figure 1 Methylation-dependent transcriptional silencing of *ASS1* in GBM. (a) Expression of novel candidate genes is upregulated by demethylation. The figure shows qPCR analysis of the indicated genes in GAMG cells treated (black) or untreated (clear) with 5'AZA. Experiments were performed in triplicate and data shown are mean fold increases (+/- 1 S.D.) in 5'AZA-treated cells relative to control cells treated with dimethylsulphoxide. (b) 5'AZA upregulates *ASS1* in GAMG but not 42MG cells. The top panel shows qPCR, the middle panel MSP and the bottom panel western blot analysis of *ASS1* in GAMG and 42MG cells with and without exposure to 5'AZA as indicated. Actin is used as a loading control for the western blot. (c) qPCR and western blot analysis of *ASS1* in primary GBM explants. qPCR was performed in triplicate and data shown are expression relative to GBM 7 (+/- 1 S.D.). (d) MSP analysis of *ASS1* CpG island in primary GBM explants. The figure shows unmethylated (U) and methylated (M) reactions for each case. Also shown are control U and M DNA samples modified in parallel with the experimental DNA samples. (e) Pyrosequencing analysis of *ASS1* CpG island in primary GBM explants. The level of methylation in individual CpG dinucleotides is indicated by the intensity of shading as shown

but without detectable methylation in the CpG island (GBM 6, 27, 25 and 41; Figures 1d and e).

ASL is silenced in primary GBM. ASS catalyses the rate-limiting step in arginine biosynthesis prompting us to ask whether expression of ASL, the next enzyme in the arginine biosynthetic pathway, is also downregulated in GBM. As no antibodies recognizing ASL protein exist, we analysed expression of ASL using qPCR. Downregulation of ASL mRNA was observed in 5/22 primary GBM cultures, results are shown for 10 primary cultures (Figure 2a). As with ASS1, there is a CpG island in the regulatory sequences of ASL (Supplementary Figure S1). Using MSP and pyrosequencing, we showed that each of the primary GBM with downregulation of ASL was methylated in the ASL CpG island (Figures 2b and c). To confirm the role of CpG island methylation, we treated cells with AZA and observed upregulation of ASL in GBM 59 (CpG island methylated) but no effect on ASL levels in GBM 6 (CpG island unmethylated). Following AZA, there was a reduction in CpG island methylation in GBM 59 (Figure 2d).

As was observed for ASS1, there were cases in which ASL mRNA was downregulated but without detectable methylation in the CpG island (GBM 16 and 41).

Methylation abrogates adaptive transcriptional upregulation of ASS1 and ASL and confers arginine auxotrophy. As ASS1 and ASL are key enzymes in the biosynthesis of arginine, we tested the effects of arginine deprivation on the growth of primary GBM cultures using the

enzyme ADI-PEG20. We first performed a detailed dose response analysis and showed that the presence of CpG island methylation in either ASS1 or ASL CpG island was associated with sensitivity to the anti-proliferative effects of ADI-PEG20 (GBM 31, 27), whereas cells in which the CpG islands of ASS1 and ASL were unmethylated were insensitive to ADI-PEG20 (GBM 16) (Figure 3c and Supplementary Table S2). Cells with methylation in both CpG islands were hypersensitive to the drug, with complete inhibition of growth at a concentration of 0.06 μ g/ml (GBM 59) (Figure 3c). For analysis of ASS1 and ASL gene expression, qPCR and western blotting were performed 48 h post treatment. ADI-PEG20 induced robust upregulation of ASS1 and ASL mRNA and ASS protein in unmethylated lines as shown in Figures 3a and b, respectively. This adaptive upregulation was absent in cells with CpG island methylation, but upregulation was readily induced in these cells by 5'AZA. These results suggest that CpG island methylation in ASS and ASL, rather than absolute expression levels *per se*, is the critical determinant of sensitivity to ADI-PEG20.

To confirm these results, a panel of GBM cell lines were similarly tested. We confirmed that both ASS1 and ASL are subject to methylation-dependent transcriptional silencing (Supplementary Figure S2) and that CpG island methylation is a critical determinant of sensitivity to ADI-PEG20 (Supplementary Figure S3 and Supplementary Table S2).

Knock down confirms the role of ASS1 in ADI-PEG20 sensitivity. To further verify the role of ASS1 in sensitivity to ADI-PEG20, we generated stable knockdown cells of ASS1

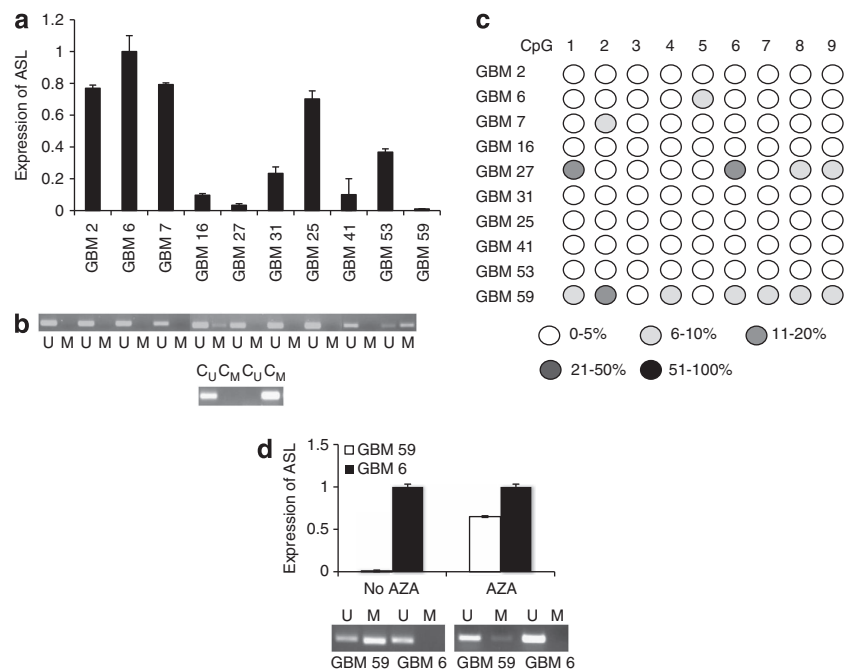


Figure 2 Methylation-dependent transcriptional silencing of ASL. (a) qPCR analysis of ASL in primary GBM explants. qPCR was performed in triplicate and data shown are expression relative to GBM 6 (± 1 SD). (b) MSP analysis of ASL CpG island in primary GBM explants. The figure shows unmethylated (U) and methylated (M) reactions for each case. Also shown are control U and M DNA samples modified in parallel with the experimental DNA samples. (c) Pyrosequencing analysis of ASL CpG island in primary GBM explants. The level of methylation in individual CpG dinucleotides is indicated by the intensity of shading as shown. (d) 5'AZA upregulates ASL in primary GBM 59 but not in primary GBM 6 cells. The top panel shows qPCR and the bottom panel MSP analysis of ASL in GBM 59 and GBM 6 cells with and without exposure to 5'AZA as indicated

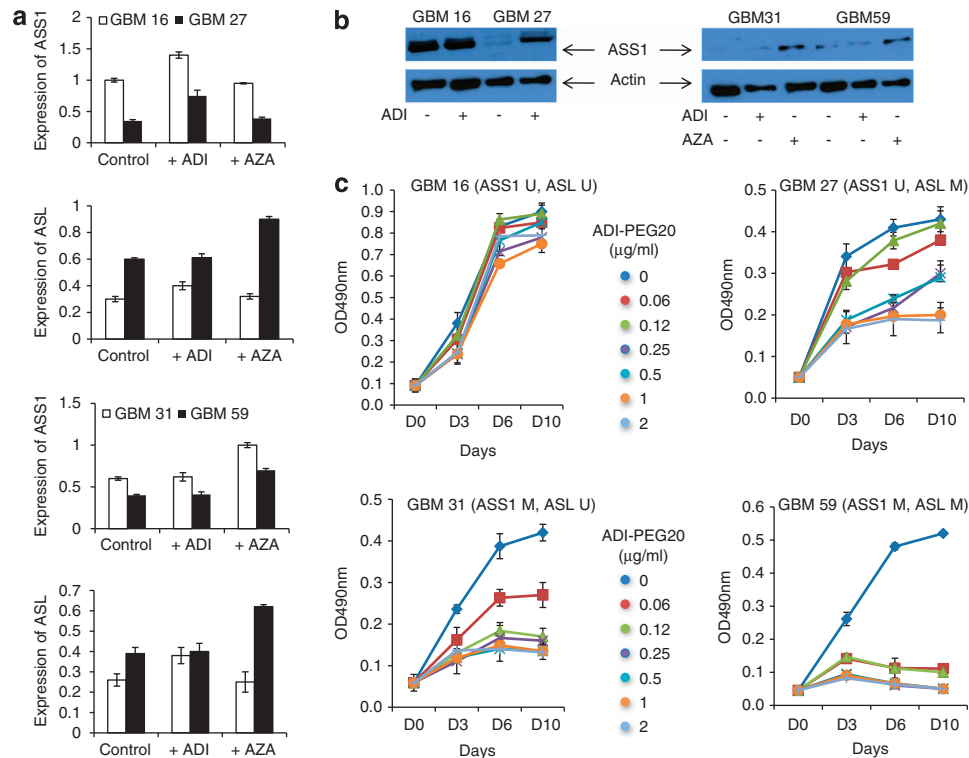


Figure 3 Methylation in the *ASS1* and *ASL* CpG islands blocks transcriptional upregulation upon arginine deprivation and confers arginine auxotrophy and sensitivity to arginine deiminase (ADI-PEG20) in primary GBM explants. (a) Arginine deprivation induces *ASS1* and *ASL* mRNA in primary GBM cells, but this is abrogated by CpG island methylation. The indicated GBM explants were grown in the presence of ADI-PEG20 (1 μ g/ml) or 5'AZA (1 μ M) as shown. RNA was harvested after 48 h and subjected to qPCR analysis of *ASS1* and *ASL* as indicated. Each experiment was performed at least twice and the values shown are means (\pm 1 SD) relative to untreated control cells. (b) Western blot analysis of ASS in primary GBM cells. The indicated primary explants were grown in the presence of ADI-PEG20 (1 μ g/ml) or 5'AZA (1 μ M) as shown. ASS levels were analysed by western blotting after 48 h. Actin is used as a control protein. (c) Dose response curves for ADI-PEG20 in primary GBM of varying CpG island methylation status. Logarithmic phase primary GBM cells were exposed to the indicated concentrations of ADI-PEG20 and proliferation assessed by measurement of SRB as described in Methods. The most sensitive tumour is GBM 59 in which both *ASS1* and *ASL* CpG islands are methylated and which is fully inhibited by 0.06 μ g/ml ADI-PEG20. By contrast, GBM16 (*ASS1* and *ASL* unmethylated) is unaffected by ADI-PEG20. GBM 27 and GBM 31 (either *ASS1* or *ASL* CpG islands methylated) show intermediate sensitivity to ADI-PEG20

using the T98G cell line. Having confirmed knock down by qPCR and western blotting (Figure 4a, upper panel), we showed that reduced levels of *ASS1* confer sensitivity to ADI-PEG20 (Figure 4a, lower panel).

Arginine auxotrophic GBM CSCs are sensitive to ADI-PEG20. The presence of CSCs in GBM is thought to be associated with resistance to temozolomide and treatment failure.^{6,28} Targeting these cells is therefore critical. Using flow cytometry, we detected a population of stem cells in the DBTRG GBM cell line (*ASL* methylated, partial sensitivity to ADI-PEG20) using the putative stem cell marker, CD133 (Figure 4b, upper panel). To test the effect of ADI-PEG20 on the CD133⁺ component, sorted cells were challenged with ADI-PEG20 and analysed for proliferation. Both populations of cells were equally inhibited in the presence of ADI-PEG20 (Figure 4b, lower panel).

Methylation of *ASS1* sensitizes cells to autophagy upon arginine deprivation. Previous studies have shown that ADI-PEG20 induces autophagy in some *ASS*-negative cell lines,^{22,29} but the relationship to epigenetic status is

unknown. As autophagy is a protective response to conditions of nutrient deprivation, we were interested to determine whether ADI-PEG20 was initially inducing an autophagic response in GBM cells. To investigate this, cell lines were exposed to ADI-PEG20 and analysed for markers of autophagy by western blotting (upregulation of Beclin 1 and the Atg genes 5 and 7, degradation of P62 and the conversion of cytosolic LC3-1 to the lipidated form LC3-11³⁰) and acridine orange staining (formation of acidic vesicular organelles). Acidic vesicular organelles are a characteristic feature of autophagy and can be detected and measured by vital staining with acridine orange, which accumulates in these acidic compartments, and is detectable as bright red fluorescence.³¹ Typical autophagic changes were detectable as early as 6 h after ADI-PEG20 treatment and progressively accumulated at 16 and 24 h in the *ASS1*-methylated line LN229 only (Figure 4c). Similarly, acidic vesicular organelles were only detected in this line and not in the unmethylated line T98G (Figure 4d). Treatment with bafilomycin A1, a specific inhibitor of vacuolar-type H⁺ ATPase, abrogated the formation of acidic vesicular organelles and no fluorescence was observed (Figure 4d).

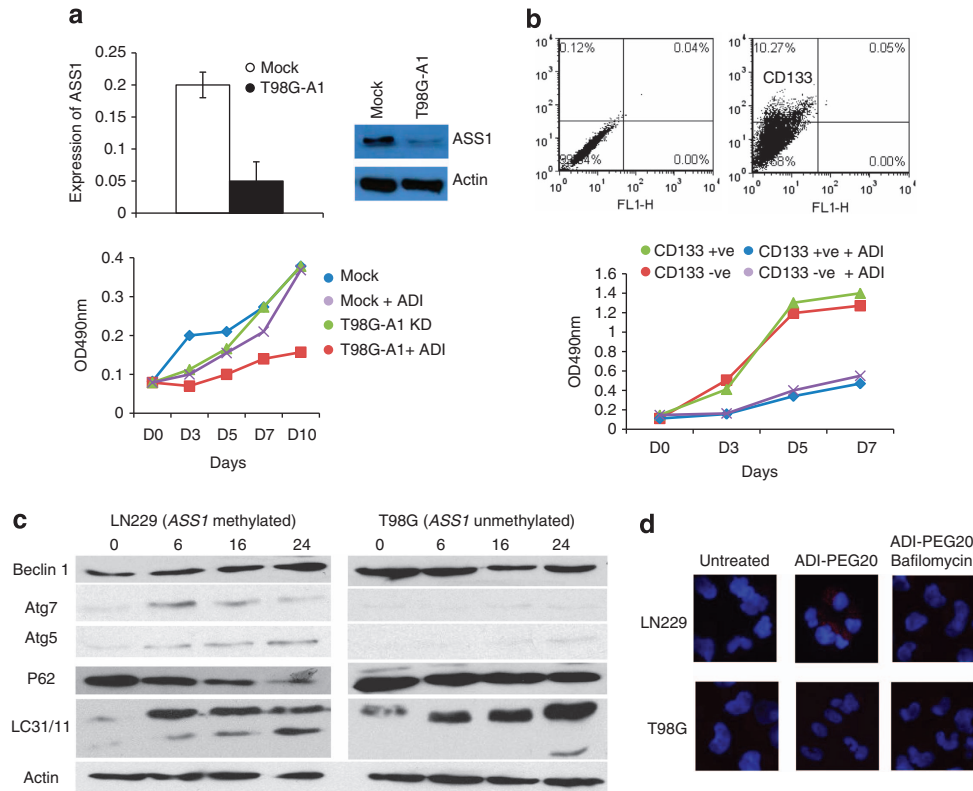


Figure 4 ADI-PEG20 kills *ASS1* knockdown cells, ASL negative CSCs and induces autophagy. (a) *ASS1* knockdown cells are sensitive to ADI-PEG20. Stable *ASS1* knockdown cells (T98G-A1) were exposed to ADI-PEG20 and analysed for proliferation as described in Methods. Cells containing empty vector were treated similarly. Upper panel confirms knock down of *ASS1* by qPCR and western blotting. T98G-A1 cells are more sensitive to killing than mock transfected cells, lower panel. (b) ADI-PEG20 kills CD133-positive GBM cells. DBTRG cells (*ASS1* unmethylated, *ASL* methylated) were sorted for CD133-positive cells (left histogram, IgG isotype control PE antibody; right histogram, anti-CD133 showing 10.27% CD133-positive cells). CD133-positive and -negative fractions were then exposed to ADI-PEG20 (1 μ g/ml) and proliferation assessed by SRB staining. CD133-positive and -negative fractions are equally sensitive to inhibition by ADI-PEG20, lower graph. (c and d) ADI-PEG20 induces autophagic markers. LN229 and T98G cells were exposed to ADI-PEG20 (1 μ g/ml) and analysed for autophagic markers by western blotting (upregulation of Beclin 1 and Atg proteins, degradation of P62 and conversion of LC3-1 to LC3-11) (c) and by acridine orange staining (formation of acidic vacuoles) in the presence or absence of bafilomycin 48 h after treatment (d). Autophagic changes are observed in the *ASS1* methylated cell line, LN229, only. Bafilomycin abrogates the formation of acidic vacuoles, which stain red in the absence of bafilomycin

Chloroquine (CQ) inhibits autophagy and accelerates ADI-PEG20 induced cell death. To test the hypothesis that ADI-PEG20 induced autophagy is (at least initially) a survival strategy for GBM cells, we investigated the effect of CQ, an inhibitor of autophagy. CQ efficiently blocked ADI-PEG20-induced p62 degradation and increased LC3-1 to LC3-11 conversion in the *ASS1*-methylated cell line LN229 (Figure 5a). These results are consistent with the fact that CQ acts late in autophagy, resulting in the accumulation of lipidated LC3-11. To further verify autophagy, stable LN229 cell lines expressing GFP-LC3 were generated to visualize autophagosome formation in real time in live cells. During autophagosome formation, GFP-LC3B is processed and recruited to the autophagosome membrane where it can be imaged as cytoplasmic puncta by high resolution fluorescence microscopy. Punctate GFP staining could be detected in ADI-PEG20-treated cells, which accumulated in the presence of CQ. This is consistent with the fact that CQ inhibits autophagic flux of LC3 (Figure 5b). No punctate staining was observed in GFP vector control cells.

To examine the effect of CQ on ADI-PEG20-induced cell death, cells were treated with either or both CQ and

ADI-PEG20 and analysed by flow cytometry for sub-G1 content using propidium iodide. CQ accelerated and enhanced ADI-PEG20-induced cell death in cells with methylation in either the *ASS1* or *ASL* CpG island as evidenced by an increase in the sub-G1 compartment (Figure 5c). By contrast, there was no effect of CQ in cells lacking methylation in the *ASS1* and *ASL* CpG islands (Figure 5c). In methylated lines, cell death was first detectable at 72 h following treatment with ADI-PEG20 alone. However, in combination with CQ, cell death could be detected at 48 h. By 72 h, CQ further increased ADI-PEG20-induced cell death (Figure 5c).

Caspase inhibitors do not prevent ADI-PEG20-induced cell death. To determine the role of caspases in ADI-PEG20-induced cell death, a caspase inhibition assay was performed. LN229 (*ASS1* methylated) and T98G (*ASS1* and *ASL* unmethylated) cells were pre-treated with the pan caspase inhibitor Z-VAD and then exposed to ADI-PEG20. Cells were then harvested for assessment of caspase- and non-caspase-mediated cell death by staining with FITC-annexin and propidium iodide. Treatment of cells with Z-VAD

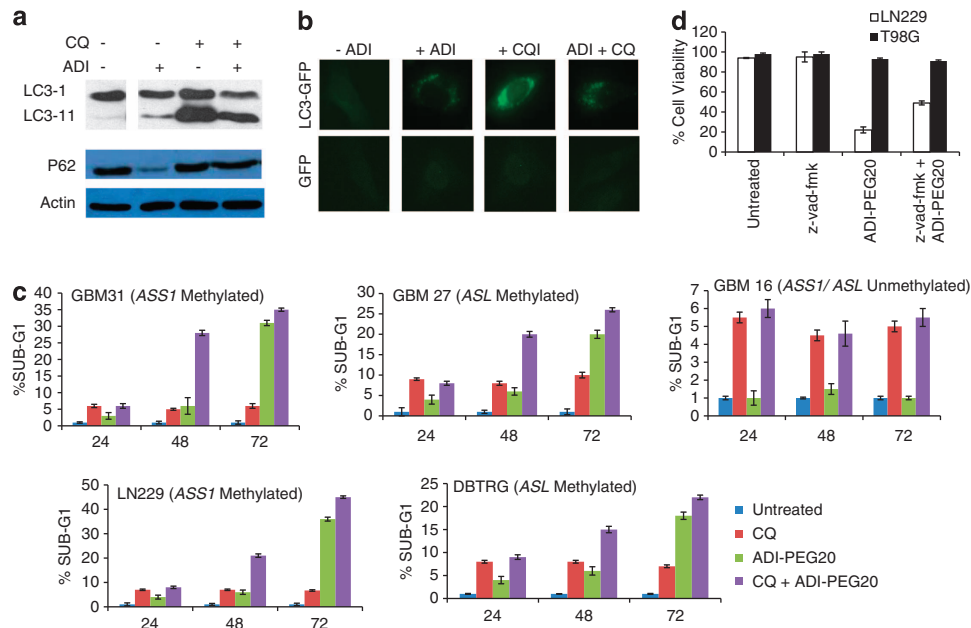


Figure 5 Caspase-independent cell death is induced by ADI-PEG20 and is accelerated by chloroquine. **(a)** CQ inhibits autophagic markers. LN229 cells were treated with 1 $\mu\text{g/ml}$ ADI-PEG20 with and without 10 $\mu\text{g/ml}$ CQ and analysed for conversion of LC3-1 to LC3-11 and degradation of P62 by western blotting 48 h post treatment. CQ inhibits degradation of P62 and prevents autophagic flux as evidenced by accumulation of the LC3-11 band. **(b)** LN229 cells stably expressing GFP-LC3 or empty GFP vector were treated as above and analysed for punctate, autophagosome-associated LC3-11 GFP by fluorescence microscopy. **(c)** Inhibition of autophagy accelerates and enhances ADI-PEG20 induced cell death. Primary and GBM cell lines were treated with 10 μM CQ, 1 $\mu\text{g/ml}$ ADI-PEG20 or in combination and analysed for sub G1 content by flow cytometry at various time points. (Primary lines – GBM 31 ASS negative, GBM 27 ASL negative, GBM 16 ASS and ASL positive; GBM cell lines – LN229 ASS negative, DBTRG ASL negative). CQ in combination with ADI-PEG20 accelerates and enhances cell death in ASS1/ASL negative lines only as evidenced by an increase in the sub-G1 compartment. The results shown are mean values from three independent experiments. **(d)** Caspase inhibitors do not prevent ADI-PEG20-induced cell death. LN229 and T98G cells were exposed to 1 $\mu\text{g/ml}$ ADI-PEG20 and analysed for sub-G1 content as above. Where indicated, the caspase inhibitor Z-VAD-fmk was added to cells 24 h before addition of ADI-PEG20. Results are expressed as the mean percentage of live cells remaining from three independent experiments. ADI-PEG20 has no effect on cell death in the unmethylated cell line, T98G but induces marked cell death (78%) in the methylated line, LN229. The percentage of cell death induced by ADI-PEG20 is only partially blocked by Z-VAD-fmk (51%)

alone had no effect on cell death in either LN229 or T98G (Figure 5d). Caspase-independent cell death was observed in LN229 (51%) but not T98G cells when pre-treated with Z-VAD in the presence of ADI-PEG20. There was a higher percentage of cell death in LN229 treated with ADI-PEG20 alone (78%), suggesting that 27% of cell death is attributable to caspases.

ASS1 and ASL are frequent targets for epigenetic inactivation in clinical cases of GBM. In order to translate these results into the clinical setting, we examined the two genes in clinical cases of human GBM using immunohistochemistry, MSP and pyrosequencing. Previous studies on ASS in melanoma, ovarian carcinoma and osteocarcinoma showed focal expression in tumour tissue. There are no published data on the expression of ASL in tumour tissue. Sixty patients (36 male, 24 female, median age 57 years) were retrospectively studied for ASS and ASL methylation and, of these cases, 55 were evaluated for ASS expression and 57 for ASL expression using a semi-quantitative scoring system as described in Methods. Representative ASS and ASL immunostaining and MSP in clinical cases are shown in Figures 6b and d. The methylation status of primary cells generated from some of these primary tumours is also shown (Figure 6d). These primary lines were stained for GFAP, a

putative astrocyte marker and H&E stained (Figure 6a). All cases were further characterized by staining for p53, IDH1 and EGFR, CD133 and MGMT methylation (data not shown).

In all, 13/55 samples were negative for ASS expression by immunohistochemistry and scored 0. These negative cases correlated well with MSP and pyrosequencing data. A further 15 cases were methylated by MSP and had pyrosequencing values >5 , an arbitrary cutoff for methylation positivity. Eleven of these cases had low ASS staining (score 1), whereas four cases exhibited strong ASS staining (score 2). These results are represented in Supplementary Table S3. Similarly for ASL, 5/57 stained negative (score 0) and correlated with methylation. A further five showed no correlation with methylation and immunohistochemistry. Eight cases were positive for both ASS1 and ASL methylation (Supplementary Table S3).

ASS1 and ASL CpG island methylation is a predictive biomarker in GBM. To determine whether methylation of ASS1 and/or ASL affects outcomes of patients, we carried out a statistical analysis as described in Methods. Median overall survival for GBM patients with unmethylated ASS1 CpG island was 496 days *versus* 309 days for patients with methylated ASS1 CpG island ($P=0.11$). Median overall survival for patients with unmethylated ASL CpG island was

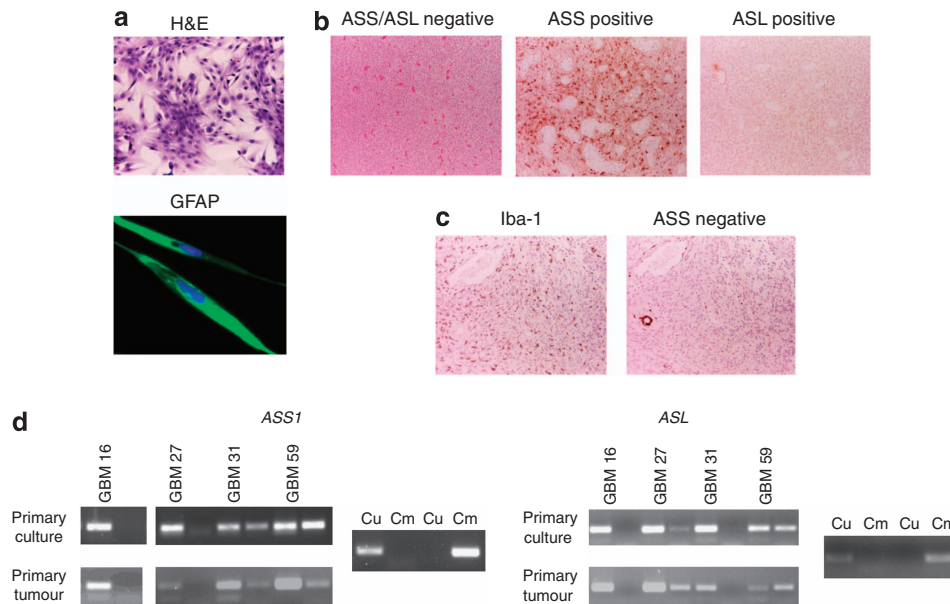


Figure 6 ASS and ASL in clinical cases of GBM. (a) Primary lines generated from tumour explants were stained for GFAP and hematoxylin and eosin. Representative examples are shown. (b) Immunohistochemistry showing ASS and ASL in clinical cases of GBM. (c) Immunohistochemical analysis for the microglial marker, Iba-1, in ASS-negative GBM. (d) MSP for *ASS1* and *ASL* CpG islands in clinical cases of GBM and primary lines generated from them. The figure shows unmethylated (U) and methylated (M) reactions for each case. Also shown are control U and M DNA samples modified in parallel with the experimental DNA samples

443 days compared with 299 days for patients with methylated *ASL* CpG island ($P=0.16$). Median overall survival for patients whose GBM showed methylation in the CpG islands of both *ASS1* and *ASL* was significantly shorter than those in whom neither CpG island was methylated or only one of the two CpG islands was methylated. Median overall survival in cases with either CpG island or none methylated = 436 days *versus* 299 days ($P=0.0468$) (Figure 7).

ASS/ASL in non-neoplastic cells. Gliomas are characterized by a high number of non-neoplastic microglial cells residing within and around the tumour. Previous studies on rat microglia showed that ASS and ASL proteins are upregulated in response to damage.²⁴ We were interested to determine the *ASS1/ASL* status of the infiltrating microglia as they could effectively provide an exogenous source of arginine for ASS/ASL-negative tumours and negate the effect of ADI-PEG20 treatment. Tissue sections were stained for Iba-1, a macrophage/microglia-specific surface antigen and for ASS. No ASS staining was observed in Iba-1-positive cells, suggesting that microglia within GBM do not/cannot upregulate the *ASS1* gene (Figure 6c).

Discussion

Despite advances in imaging and surgical techniques and the use of temozolomide, GBM remains a universally and rapidly fatal cancer, affecting patients of all ages. As such, the requirement for novel therapeutic strategies is clear and pressing. Here we show that *ASS1* and *ASL*, encoding the two key enzymatic components of the arginine biosynthetic pathway, are epigenetically regulated in glial brain tumours,

and we provide evidence that targeting of this pathway is a novel therapeutic strategy for a subset of patients with this disease. The importance of metabolic changes in brain tumours has been recently illustrated by the detection of gain-of-function mutations in isocitrate dehydrogenase in oligodendrogliomas and the secondary GBM, which develop from a subset of them.³² The present data show that arginine metabolism is disrupted in a proportion of GBM, further emphasizing that abnormalities in fundamental metabolic pathways are a major feature of this disease. A key element of our study is the use of low passage primary cultures of GBM cells. These cultures are established in culture on the day of surgical debulking, closely resemble the primary GBM from which they were established in both expression and methylation of *ASS1* and *ASL* and in their response to arginine deprivation, analogous to established GBM cell lines and are clearly a more appropriate model for pharmacological studies than cell lines that have been maintained in culture for many years.

We initially identified *ASS1* as a transcriptionally down-regulated gene in studies using the demethylating agent 5'AZA to reverse methylation. A number of genes were upregulated that have not been previously described as epigenetically regulated in brain tumours specifically or, more generally, in human cancer. These include, among others, amino butyrate amino transferase (*ABAT*), *EFEMP1* and *ZNF365*. The significance of silencing of these genes and their role (if any) in the pathogenesis of GBM awaits further analysis.

We show, using two independent techniques (MSP and pyrosequencing), that the *ASS1* CpG island is aberrantly methylated in 30% and the *ASL* CpG island in 22% of GBM. Only a single study has previously demonstrated

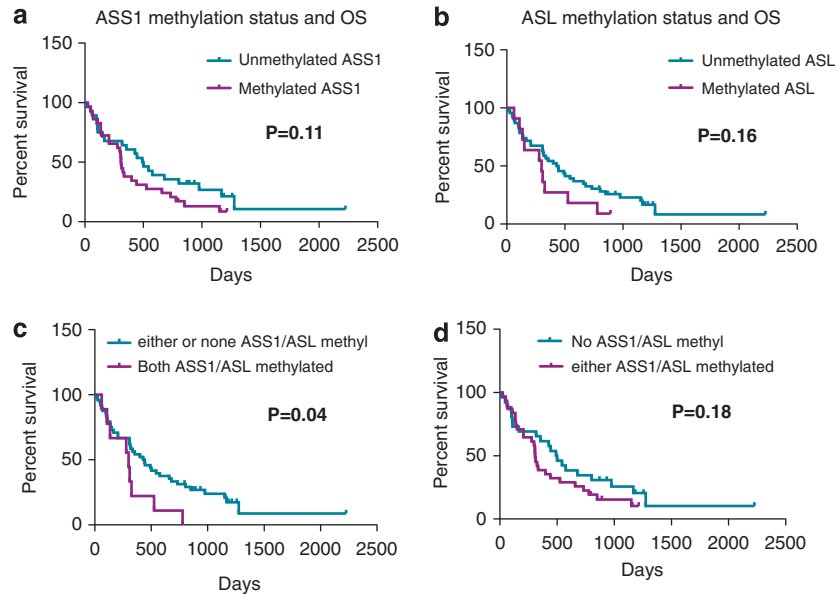


Figure 7 Methylation of *ASS1* and *ASL* CpG island is a predictive biomarker in GBM. To determine whether methylation of *ASS1* and/or *ASL* affects outcomes of patients, Kaplan–Meier curves were used to estimate the probabilities of survival and the log-rank test to assess the statistical significance of differences in event rates using Prism 5. (a) Median overall survival (OS) for GBM patients with unmethylated *ASS1* CpG island was 496 days *versus* 309 days for patients with methylated *ASS1* CpG island ($P = 0.11$). (b) Median OS for patients with unmethylated *ASL* CpG island was 443 days compared with 299 days for patients with methylated *ASL* CpG island ($P = 0.16$). (c) Median OS for patients whose GBM showed methylation in the CpG islands of both *ASS1* and *ASL* was significantly shorter than those in whom neither CpG island was methylated or only one of the two CpG islands was methylated ($P = 0.0468$). (d) Median OS in cases with either CpG island or none methylated = 436 days *versus* 299 days ($P = 0.18$)

methylation-dependent transcriptional silencing of *ASS1* in neoplasia, this in platinum-resistant epithelial ovarian cancer,²¹ but no previous study has examined expression and epigenetic regulation of *ASL*. As such, ours is, to the best of our knowledge, the first demonstration of epigenetic regulation of this gene in human neoplasia. Silencing of *ASS1* and *ASL* implies strong selective pressure to downregulate the arginine biosynthetic pathway in GBM. Moreover, we have shown that simultaneous methylation in the CpG islands of both *ASS1* and *ASL* occurs in 14% of GBM cases in our series, further emphasizing that strong selective pressure against cancer cells expressing the two genes must operate in GBM.

In GBM cells lacking CpG island methylation, the mRNA of both *ASS1* and *ASL* is upregulated by exposure to ADI-PEG20 and a similar upregulation is seen when cells are grown in arginine-free culture medium (data not shown). Upregulation of biosynthetic enzymes has been long recognized as a normal physiological response to nutritional deprivation, for example, under conditions of starvation.^{28,29} Here we show that CpG island methylation blocks the adaptive transcriptional response to arginine deprivation and it is this, rather than absolute expression levels of *ASS* or *ASL*, that is the critical determinant of cellular sensitivity to ADI-PEG20.

We demonstrate herein that ADI-PEG20 kills GBM cells with *ASS/ASL* CpG island methylation predominantly independently of caspase activation, suggesting that failure of apoptosis will not be a barrier to successful therapy with ADI-PEG20. Furthermore, inhibiting autophagy by CQ markedly accelerated cell death by ADI-PEG20, implying that autophagy triggered by ADI-PEG20 is initially a protective response.

Trials of the clinical formulation of ADI-PEG20 are in progress in advanced hepatocellular carcinoma, relapsed or refractory small cell lung cancer and malignant pleural mesothelioma (<http://clinicaltrials.gov>). A number of factors from our work suggest that clinical trial of ADI-PEG20 in GBM is merited. First, a major advantage of the proposed study in GBM is that patients whose cancers exhibit methylation of *ASS1* and/or *ASL* can be further pre-tested for sensitivity to ADI-PEG20 *in vitro* using primary cultures to inform the physician of likely treatment response. Such primary cultures can be established efficiently, rapidly and with a high probability of success from tissue obtained at biopsy or primary debulking. Importantly, sufficient cells to allow predictive pharmacological testing are available within a credible time scale after surgery to inform the use of ADI-PEG20. Second, the extremely unfavourable prognosis for GBM patients correlates with intrinsic resistance to apoptosis of GBM cells.^{4,5} Clinical trials of CQ in combination with standard therapy showed some improvement in the survival of GBM patients.^{30,31} Interestingly, the CQ derivatives quina-crine and mefloquine show superior blood/brain penetration in comparison to CQ and are more potent *in vitro* than CQ in killing GBM cells,³³ and we propose that combinations of ADI-PEG20 with CQ or CQ derivatives merit consideration for clinical trial in appropriate GBM patients. Third, recurrence of GBM after therapy has been attributed to the presence of chemo-/radio-resistant CD133⁺ CSCs.⁶ We have shown in this work that in cells with methylated *ASL*, CD133⁺ GBM cells are growth inhibited by ADI-PEG20 with the same efficiency as CD133⁻, implying that the presence of chemo-/radio-resistant CD133⁺ cells will not be a barrier to effective therapy with ADI-PEG20 *in vivo*. Fourth, a major factor limiting

effective management of GBM is the presence of the blood/brain barrier, which may act to prevent efficient delivery of chemotherapy into the brain. Clearly, as ADI-PEG20 exerts its therapeutic effect by depletion of peripheral blood arginine, passage across the blood/brain barrier is not required for therapeutic efficacy of this agent. Based on these observations, we believe that clinical trial of arginine-deprivation therapy with CQ or CQ derivative compounds is warranted in GBM. CpG island methylation of either *ASS1* or *ASL*, but especially of *ASS1* and *ASL* simultaneously, was associated with particularly poor outcomes in patients treated with the current gold-standard therapy of radiotherapy and temozolomide. We have shown herein that GBM with CpG island of methylation of both *ASS1* and *ASL* are hypersensitive to ADI-PEG20, implying that arginine depletion may be an appropriate therapy for patients with particularly poor prognosis disease.

In conclusion, the data we present here identify a new metabolic defect in GBM cells and suggest a novel therapeutic strategy, which circumvents many of the traditional barriers to effective management of this universally fatal malignancy.

Methods

Cell lines, primary cultures and clinical cases. Primary GBM cultures were established from fresh tumours and maintained in DMEM/ F12 (1:1) supplemented with 10% (foetal bovine serum). In brief, fresh tumour material was washed in RPMI/F12 (1:1) and minced through a cell strainer to obtain a single-cell suspension. Contaminating red blood cells were disrupted using sterile dH₂O before cells were transferred to fresh growth medium. Primary cells were expanded and early passage numbers were frozen in liquid N₂ for analysis at a later time point. Glioblastoma cell lines were obtained from the German tissue bank (DSMZ) unless otherwise specified and maintained in RPMI (DBTRG), DMEM (GAMG, SNB19, U87, U118, CCF, LN229), MEM (8MG, T87G), DMEM/ F12 (1:1) (MO59J, MO59K) or MEM/RPMI 1:1 (42MG) supplemented with 10% foetal bovine serum (All purchased from Invitrogen, Paisley, UK) and 2 mmol/l L-glutamine (Sigma-Aldrich, Dorset, UK).

Sixty GBM cases selected from the Brain Tumour Registry at Imperial College were selected for detailed analysis of enzymes in the arginine biosynthetic pathway. Detailed clinical history, pre- and post-operative imaging and follow-up were available in 60 cases. In all, 24 patients were female and 36 male with mean age 58 years and 7 months (range = 31 years and 1 month–83 years 11 months; median 59 years 7 months). In each case, original H&E-stained sections were re-examined to confirm the diagnosis, and the most representative samples were used for immunohistochemical stains. Samples were obtained from surgical debulking rather than stereotactic biopsies in order to examine as much tumour tissue as possible. As such, we chose only supratentorial GBMs because gross total debulking is not achievable in tumours occurring in the sub-cortical grey matter, cerebellum, brainstem and spinal cord. Finally, we selected patients with a clinical history consistent with a *de novo* GBM because almost all patients with secondary GBM received treatment before debulking.

Methylation reversal. Cell lines and primary cultures were grown in the presence of 5 μ M 5'AZA (Sigma-Aldrich) for 7 days. Fresh AZA was added with every medium change and supplemented with 300 nM Trichostatin A (Sigma-Aldrich) for the last 16 h of culture. Controls cells were treated with dimethylsulphoxide.

Immunohistochemistry. Paraffin-embedded blocks were cut into 5 μ m sections and dewaxed in xylene followed by rehydration in a standard alcohol series. Antigen retrieval (for ASS) was achieved by pressure cooking for 20 min in citrate buffer (pH 6.0), followed by blocking of endogenous peroxidase in 0.3% H₂O₂. Antibodies to ASS (BD Transduction, monoclonal, 25/ASS, 1:500, Oxford, UK), ASL (Abnova, monoclonal, clone 4C5-1F2, 1:200, Heidelberg, Germany) and Iba-1 (rabbit polyclonal antibody, Wako, Osaka, Japan, 1:200) were added and incubated overnight at 4 °C and developed using the Super Sensitive Polymer HRP Detection System (BioGenex Laboratories, Inc., Fremont, CA, USA).

Expression of ASS/ASL was assessed semi-quantitatively where negative tumours are defined as negative with expression ranging between 0–5% (score 0) and diffuse (score 2) those showing expression in 75% or more tumour cells. Anything in between negative and diffuse was defined focal and scored 1.

Analysis of gene expression *in vitro*. For qPCR, total RNA was prepared from log phase cell lines and primary GBM cultures using the EZNA isolation kit total RNA 1 according to the manufacturer's instructions (VWR, Leicester, UK). cDNA was synthesized from 1 μ g of total RNA using anchored oligo(dT) primers and MMLV reverse transcriptase (Invitrogen).

Quantitative real-time reverse transcription-PCR (qPCR). All primers were designed using Primer Express version 1.5a software (Life Technologies Ltd, Paisley, UK). qPCR was performed with Syber Green fast mix (Quanta Biosciences, Gaithersburg, MD, USA) using the Biorad CFX96 Detection System instrument and software (Bio-Rad Laboratories Ltd, Hemel Hempstead, UK). In all, 0.5 μ l cDNA was used per 20 μ l reaction with the following cycling conditions: an initial denaturation at 95 °C for 3 min was followed by 40 cycles of 95 °C for 10 s, 55 °C for 30 s and 72 °C for 10 s. A melt curve analysis was included as the final step, which consisted of temperature increments of 55–95 °C. Each sample was analysed in triplicate and normalized to GAPDH. Primer sequences for qPCR are given in Supplementary Table S1.

Western blot analysis. Whole-cell extracts were made using RIPA buffer and the protein concentration of lysates estimated using a Bio-Rad Protein Assay kit (Bio-Rad Laboratories Ltd, Hertfordshire, UK). Also, 10 μ g cell extract was run on a 10% SDS-acrylamide gel and transferred to a nylon membrane. The membrane was blocked for 2 h at room temperature (PBS with 0.1% Tween (PBST) and 5% milk powder) and probed using appropriate primary antibodies (ASS1, clone 25; BD Biosciences, Oxford, UK, 1:2000 dilution, autophagy antibody sampler kit, Cell Signaling Technology, Danvers, MA, USA) in 0.1% Tween (PBST) and 5% milk powder overnight at 4 °C. After washing with 0.1% Tween (PBST), the membrane was incubated in 0.1% Tween (PBST) and 5% milk powder with a horseradish peroxidase-conjugated secondary antibody (1:2000 dilution, room temperature for 1 h). The secondary antibody was detected using the ECL Plus Western Blotting Reagent (GE Healthcare, Life Sciences, Buckinghamshire, UK).

Methylation analysis. Methylation of the *ASS1* and *ASL* CpG islands was analysed by MSP and quantitative pyrosequencing. Full maps of the *ASS1* and *ASL* CpG islands are presented in Supplementary Figure S1. Primers for MSP were designed using MethPrimer software. Primer locations are shown in Supplementary Figure S1 and sequences are listed in Supplementary Table S1. Primers were designed to cover the entire region of the CpG island but only sets 1, 4, 5 and 7 were used for analysis of methylation (Supplementary Figure S1).

Bisulphite modification and MSP. Bisulphite conversion of genomic DNA was carried out using the Zymo EZ DNA methylation kit (Genetix Ltd, Hampshire, UK). This process converts unmethylated cytosine residues to uracil, whereas methylated cytosine residues remain unchanged. MSP was then carried out to determine the methylation status of *ASS1* and *ASL*. In all, 5 μ l of bisulphite-modified DNA was used as templates for PCR reactions with primers specific for methylated or unmethylated sequences. CpGenome Universal Methylated DNA and CpGenome Universal Unmethylated DNA were used as positive and negative controls, respectively. PCR conditions were as follows: 8 cycles of 95 °C for 2 min, 51.7 °C for 30 s and 72 °C for 30 s were followed by 32 cycles of 95 °C for 30 s, 51.7 °C for 30 s and 72 °C for 30 s, then a final extension at 72 °C for 5 min. PCR products were electrophoresed through 2% agarose gels, stained with ethidium bromide and visualized using a transilluminator.

Analysis of CpG methylation by pyrosequencing. Bisulphite-modified genomic DNA (see above) was used as the template in pyrosequencing. Modified DNA was then subjected to bisulphite sequencing. Biotage Sample Prep kit and primers designed to amplify a 145 bp fragment across the CpG island of *ASS1* and *ASL* genes were optimized for software dedicated to methylation analysis. After pyrosequencing, the analysis was performed using PyromarkID Software (Biotage, Uppsala, Sweden). *ASS1* forward 5'-TGTGTTTATAATTTGGG ATGG-3' and reverse 5'-GGGTTTAGAGGAGGAGG-3' primers, *ASL* forward 5'-AGGATTGGAGGATGGAGGTAA-3' and reverse 5'-CCACTAACCAAACTTTTCT AAC-3' primers. Annealing temperatures were 54 °C for *ASS1* and 58 °C for *ASL*.

Sensitivity of GBM cells to ADI-PEG20. Cell proliferation was determined at various time points using the sulphorodamine B (SRB) assay (Sigma-Aldrich). ADI-PEG20 was obtained from Polaris Pharmaceuticals Inc. (San Diego, CA, USA). Arginine-free medium was purchased from MP Biomedicals (Cambridge, UK). Cells were seeded in triplicate in 96-well plates at a density of 4×10^3 or 4×10^4 cells per well for cell lines or primary lines, respectively. Twenty-four hours after seeding, the cells were washed 3 times in PBS and cultured in medium containing varying concentrations of ADI-PEG20 (0–2 $\mu\text{g/ml}$) or in arginine-free medium supplemented with 1 mM citrulline and 2% dialysed FCS for various time points. Cells were fixed with 10% tri-chloroacetate for at least 1 h at 4 °C, washed with distilled water and allowed to dry before being stained with 0.4% SRB. The unbound SRB was washed with 0.1% acetic acid and the plates allowed to air dry. Bound SRB was dissolved in 10 mMol/l Tris pH 10.5 and absorbances read at 495 nm.

Caspase inhibition assay. GBM cell lines were seeded at a density of 1.5×10^5 cells per well in 6-well tissue culture-treated plates. Once cells had attached, they were then treated with or without 50 μM Z-VAD-fmk (Bachem, Switzerland) for 24 h in order to inhibit caspase activity. Wells were then treated in the following manner: control (untreated $-/+$ Z-VAD; citrulline 1 mM $-/+$ Z-VAD; ADI-PEG20 (0.1 $\mu\text{g/ml}$ $-/+$ Z-VAD). Cells were then left for 48 h under standard culture conditions and harvested for assessment of caspase and non-caspase-mediated cell death. Floating and attached cells (removed by trypsinisation) were then processed for flow cytometric analysis using the Annexin V-FITC Apoptosis Detection kit (Calbiochem, Nottingham, UK). Flow cytometric analysis was carried out using a Coulter EPICS flow cytometer (Beckman Coulter (UK) Ltd, High Wycombe, UK) with FL1 for FITC-annexin staining and FL3 for propidium iodide staining. Samples were analysed in duplicate and the experiments were set up on three separate occasions.

Inhibition of autophagy. Cells were treated with 10 μM CQ, 1 $\mu\text{g/ml}$ ADI-PEG20 or both for 24, 48 and 72 h. Cells were harvested, washed in PBS and resuspended in 500 ml PBS and fixed by the addition of 2 ml of cold 90% methanol for at least 2 h. After fixing, cells were washed twice in PBS and then re-suspended in 300 μl of PBS containing 1 $\mu\text{g/ml}$ propidium iodide and 10 mg/ml RNaseA and then analysed by flow cytometry for sub-G1 population.

ASS1 knockdown. Short hairpin RNA (shRNA) sequences targeting ASS1 were cloned into the pSilencer 4.1-CMVpuro vector (Ambion, Life Technologies Ltd). Sequences were designed by Ambion and supplied by Invitrogen (Supplementary Table S1). Control vector expressing an shRNA sequence that does not target any known human gene was used as a negative control in experiments. T98G, U118 and 42MG cells were transfected with shRNA-expressing vectors using Lipofectamine 1000 (Invitrogen). Stable pooled populations of transfectants were obtained following selection with 1 $\mu\text{g/ml}$ puromycin for 3–4 weeks.

Generation of stable GFP-LC3 cells. LN229 cells were transfected with GFP-LC3 (CBA-401) expression vector or empty vector (Cambridge Bioscience, Cambridge, UK). Stable pools of transfectants were obtained following selection with 800 $\mu\text{g/ml}$ of G418 for 3–4 weeks. These were expanded and stored in LN2 until required.

Flow cytometry for CD133 expression. For analysis of CD133 expression and cell sorting by flow cytometry, live cells were trypsinised, washed with cold PBS/1%FCS (wash buffer) and re-suspended at a density of 1×10^6 cells/ml in wash buffer. In all, 1×10^5 cells were incubated with 100 μl anti-CD133 antibody or mouse IgG1 isotype matched control (Miltenyl Biotech Ltd (Surrey, UK), diluted 1:100 in wash buffer) for 1 h at 4 °C. After the incubation period, cells were washed twice in wash buffer incubated with 100 μl goat-anti-mouse FITC (Sigma-Aldrich) diluted 1:100 in wash buffer. Finally cells were washed twice in wash buffer and re-suspended in 500 μl PBS/FCS before being analysed by flow cytometry and sorted for CD133-positive and -negative cells.

Statistics. Kaplan–Meier curves were used to estimate the probabilities of survival and time to progression and the log-rank test to assess the statistical significance of differences in event rates using Prism 5 (GraphPad software, Inc., La Jolla, CA, USA).

Written informed consent was received from the participants before inclusion in the study.

Conflict of Interest

The authors declare no conflict of interest.

Acknowledgements. This work was supported by the Brain Tumour Research Campaign (BTRC) charity.

- Gurney JG, Kadan-Lottick N. Brain and other central nervous system tumors: rates, trends, and epidemiology. *Curr Opin Oncol* 2001; **13**: 160–166.
- Preusser M, de Ribaupierre S, Wöhler A, Erridge SC, Hegi M, Weller M *et al*. Current concepts and management of glioblastoma. *Ann Neurol* 2011; **70**: 9–21.
- Clarke J, Butowski N, Chang S. Recent advances in therapy for glioblastoma. *Arch Neurol* 2010; **67**: 279–283.
- Ziegler DS, Kung AL, Kieran MW. Anti-apoptosis mechanisms in malignant gliomas. *J Clin Oncol* 2008; **26**: 493–500.
- Ziegler DS, Wright RD, Kesari S, Lemieux ME, Tran MA, Jain M *et al*. Resistance of human glioblastoma multiforme cells to growth factor inhibitors is overcome by blockade of inhibitor of apoptosis proteins. *J Clin Invest* 2008; **118**: 3109–3122.
- Liu Q, Nguyen DH, Dong Q, Shitaku P, Chung K, Liu OY *et al*. Molecular properties of CD133⁺ glioblastoma stem cells derived from treatment-refractory recurrent brain tumors. *J Neurooncol* 2009; **94**: 1–19.
- Kögel D, Fulda S, Mittelbronn M. Therapeutic exploitation of apoptosis and autophagy for glioblastoma. *Anticancer Agents Med Chem* 2010; **10**: 438–449.
- Lefranc F, Facchini V, Kiss R. Proautophagy drugs: a novel means to combat apoptosis-resistant cancers, with a special emphasis on glioblastomas. *Oncologist* 2007; **12**: 1395–1403.
- Lefranc F, Kiss R. Autophagy, the Trojan horse to combat glioblastomas. *Neurosurg Focus* 2006; **20**: E7.
- Kanzawa T, Germano IM, Komata T, Ito H, Kondo Y, Kondo S. Role of autophagy in temozolomide-induced cytotoxicity for malignant glioma cells. *Cell Death Differ* 2004; **11**: 448–457.
- Clarke PG. Developmental cell death: morphological diversity and multiple mechanisms. *Anat Embryol (Berl)* 1990; **181**: 195–213.
- Yang Z, Klionsky DJ. Mammalian autophagy: core molecular machinery and signaling regulation. *Curr Opin Cell Biol* 2010; **22**: 124–131.
- Haines RJ, Pendleton LC, Eichler DC. Argininosuccinate synthase: at the center of arginine metabolism. *Int J Biochem Mol Biol* 2011; **2**: 8–23.
- Gong H, Zölzer F, von Recklinghausen G, Havers W, Schweigerer L. Arginine deiminase inhibits proliferation of human leukemia cells more potently than asparaginase by inducing cell cycle arrest and apoptosis. *Leukemia* 2000; **14**: 826–829.
- Ensor CM, Holsberg FW, Bomalaski JS, Clark MA. Pegylated arginine deiminase (ADI-SS PEG20,000 mw) inhibits human melanomas and hepatocellular carcinomas *in vitro* and *in vivo*. *Cancer Res* 2002; **62**: 5443–5450.
- Yoon C-Y, Shim Y-J, Kim E-H, Lee JH, Won NH, Kim JH *et al*. Renal cell carcinoma does not express argininosuccinate synthetase and is highly sensitive to arginine deprivation via arginine deiminase. *Int J Cancer* 2007; **120**: 897–905.
- Bowles TL, Kim R, Galante J, Parsons CM, Virudachalam S, Kung HJ *et al*. Pancreatic cancer cell lines deficient in argininosuccinate synthetase are sensitive to arginine deprivation by arginine deiminase. *Int J Cancer* 2008; **123**: 1950–1955.
- Kim RH, Coates JM, Bowles TL, McNeerney GP, Sutcliffe J, Jung JU *et al*. Arginine deiminase as a novel therapy for prostate cancer induces autophagy and caspase-independent apoptosis. *Cancer Res* 2009; **69**: 700–708.
- Delage B, Fennell DA, Nicholson L, McNeish I, Lemoine NR, Crook T *et al*. Arginine deprivation and argininosuccinate synthetase expression in the treatment of cancer. *Int J Cancer* 2010; **126**: 2762–2772.
- Kelly MP, Jungbluth AA, Wu BW, Bomalaski J, Old LJ, Ritter G. Arginine deiminase PEG20 inhibits growth of small cell lung cancers lacking expression of argininosuccinate synthetase. *Br J Cancer* 2011; **106**: 324–332.
- Nicholson LJ, Smith PR, Hiller L, Szlosarek PW, Kimberley C, Sehoul J *et al*. Epigenetic silencing of argininosuccinate synthetase confers resistance to platinum-induced cell death but collateral sensitivity to arginine auxotrophy in ovarian cancer. *Int J Cancer* 2009; **125**: 1454–1463.
- Savaraj N, You M, Wu C, Wangpaichitr M, Kuo MT, Feun LG. Arginine deprivation, autophagy, apoptosis (AAA) for the treatment of melanoma. *Curr Mol Med* 2010; **10**: 405–412.
- Wheatley DN. Arginine deprivation and metabolomics: important aspects of intermediary metabolism in relation to the differential sensitivity of normal and tumour cells. *Semin Cancer Biol* 2005; **15**: 247–253.
- Bizzoco E, Faussone-Pellegrini MS, Vannucchi MG. Activated microglia cells express argininosuccinate synthetase and argininosuccinate lyase in the rat brain after transient ischemia. *Exp Neurol* 2007; **208**: 100–109.
- Etcheverry A, Aubry M, de Tayrac M, Vauleon E, Boniface R, Guenet F *et al*. DNA methylation in glioblastoma: impact on gene expression and clinical outcome. *BMC Genomics* 2010; **11**: 701.
- Stupp R, Hegi ME, Mason WP, van den Bent MJ, Taphoorn MJ, Janzer RC *et al*. Effects of radiotherapy with concomitant and adjuvant temozolomide versus radiotherapy alone on

- survival in glioblastoma in a randomised phase III study: 5-year analysis of the EORTC-NCIC trial. *Lancet Oncol* 2009; **10**: 459–466.
27. Weller M, Stupp R, Reifenberger G, Brandes AA, van den Bent MJ, Wick W *et al*. MGMT promoter methylation in malignant gliomas: ready for personalized medicine? *Nat Rev Neurol* 2010; **6**: 39–51.
28. Fafouroux P, Bruhat A, Jousse C. Amino acid regulation of gene expression. *Biochem J* 2000; **351**(Pt 1): 1–12.
29. Chaveroux C, Lambert-Langlais S, Cherasse Y, Averous J, Parry L, Carraro V *et al*. Molecular mechanisms involved in the adaptation to amino acid limitation in mammals. *Biochimie* 2010; **92**: 736–745.
30. Briceño E, Reyes S, Sotelo J. Therapy of glioblastoma multiforme improved by the antimutagenic chloroquine. *Neurosurg Focus* 2003; **14**: e3.
31. Briceño E, Calderon A, Sotelo J. Institutional experience with chloroquine as an adjuvant to the therapy for glioblastoma multiforme. *Surg Neurol* 2007; **67**: 388–391.
32. Parsons DW, Jones S, Zhang X, Lin JC, Leary RJ, Angenendt P *et al*. An integrated genomic analysis of human glioblastoma multiforme. *Science* 2008; **321**: 1807–1812.
33. Geng Y, Kohli L, Klocke BJ, Roth KA. Chloroquine-induced autophagic vacuole accumulation and cell death in glioma cells is p53 independent. *Neuro Oncol* 2010; **12**: 473–481.



Cell Death and Disease is an open-access journal published by Nature Publishing Group. This work is licensed under the Creative Commons Attribution-NonCommercial-No Derivative Works 3.0 Unported License. To view a copy of this license, visit <http://creativecommons.org/licenses/by-nc-nd/3.0/>

Supplementary Information accompanies the paper on Cell Death and Disease website (<http://www.nature.com/cddis>)